Published in final edited form as:
ACS Chem Biol. 2007 September 21; 2(9): 625–634. doi:10.1021/cb7001126.

Design of Cyclic Peptides That Bind Protein Surfaces with Antibody-Like Affinity

Steven W. Millward[†], **Stephen Fiacco**[‡], **Ryan J. Austin**[‡], and **Richard W. Roberts**[‡,*]

[‡]Department of Chemistry, Chemical Engineering, and Biology, University of Southern California, 3710 McClintock Avenue, Los Angeles, California 90089-1211

[†]Division of Chemistry and Chemical Engineering, California Institute of Technology, Pasadena, California 91125

Abstract

There is a pressing need for new molecular tools to target protein surfaces with high affinity and specificity. Here, we describe cyclic messenger RNA display with a trillion-member covalent peptide macrocycle library. Using this library, we have designed a number of high-affinity, redox-insensitive, cyclic peptides that target the signaling protein Gαi1. In addition to cyclization, our library construction took advantage of an expanded genetic code, utilizing nonsense suppression to insert *N*-methylphenylalanine as a 21st amino acid. The designed macrocycles exhibit several intriguing features. First, the core motif seen in all of the selected variants is the same and shares an identical context with respect to the macrocyclic scaffold, consistent with the idea that selection simultaneously optimizes both the cyclization chemistry and the structural placement of the binding epitope. Second, detailed characterization of one molecule, cyclic Gαi binding peptide (cycGiBP), demonstrates substantially enhanced proteolytic stability relative to that of the parent linear molecule. Third and perhaps most important, the cycGiBP peptide binds the target with very high affinity ($K_i \approx 2.1$ nM), similar to those of many of the best monoclonal antibodies and higher than that of the βγ heterodimer, an endogenous Gαi1 ligand. Overall the work provides a general route to design novel, low-molecular-weight, high-affinity ligands that target protein surfaces.

Although networks of protein–protein interactions control function inside cells, it is increasingly clear that many of these players cannot be targeted using traditional druglike molecules (1). High-affinity, high-specificity ligands targeting protein surfaces are thus of considerable interest as tools for chemical genetics, as potential lead/surrogate compounds, and as new drugs. Nanotechnology could also greatly benefit from such molecules, particularly robust, inexpensive, low-molecular-weight ligands that could replace monoclonal antibodies (2). Designing these ligands still remains a significant challenge despite the tremendous advances in structural biology and computational chemistry.

Our laboratory has been working to design new peptide ligands that target heterotrimeric G-protein signaling. We have previously used messenger RNA (mRNA) display (3) to isolate new linear peptides that target Gαi1 (4–6). Gαi1 is a member of the Gα subunit family and serves as a molecular router, connecting the cell-surface G-protein-coupled receptors (GPCR) to down-stream effector pathways (see ref 7 for a review of GPCR signaling). Gα subunits function by collaboration with the Gβγ heterodimer and a transmembrane receptor. The Gαβγ heterotrimer associates with the cytosolic portion of GPCRs with GDP bound in the nucleotide pocket of Gα. Extracellular ligand binding to the GPCR results in

*Corresponding author, richrob@usc.edu.

intracellular exchange of bound GDP for GTP, dissociation of Gα from Gβγ, and activation or inhibition of downstream effectors. Hydrolysis of GTP on the Gα subunit results in reformation of the stable heterotrimer and termination of the signal.

GPCRs are clinically important, and a large fraction of marketed drugs target these receptors (8). Additionally, a number of disease states are linked to aberrant Gα expression or Gα mutations, including McCune–Albright syndrome; pituitary, thyroid, and adrenal tumors (9); and ovarian stromal and adrenal cortex tumors (10). The selective modulation of specific Gα subclasses by druglike compounds would facilitate the dissection of G-protein control circuits and provide starting points for the development of G-protein-targeted therapeutics.

Peptide ligands represent one route to target Gαi1 (Table 1). Examples include the natural GoLoco motif found in Arg-Gly-Ser domains (K_d = 82 nM) (5, 11), the KB-752 peptide isolated by phage display (16 amino acids; K_d = 3.9 μM) (12), and the R6A peptide (and related sequences) isolated by mRNA display (17 amino acids; K_d = 60 nM) (5). These peptides are potent *in vitro* ligands and can function *in vivo* when microinjected into cells (6, 13). On the other hand, these peptides are unlikely to be functional as traditional drugs *in vivo* because of their (i) proteolytic susceptibility and (ii) poor cell membrane permeability traditionally associated with linear peptides.

The peptidic products of non-ribosomal peptide synthetases are examples of peptides that can act as drugs (reviewed in ref 14). Cyclosporin, a cyclic 11-residue peptide produced commercially by the fungus *Beauveria nivea* acts as a potent orally bioavailable immunosuppressant (15). The enhanced proteolytic stability and cell permeability of cyclosporin are likely the result of both unnatural *N*-methyl amino acids (16, 17) and macrocyclization (18, 19). Using this molecule as a guide, we reasoned that ribosomally synthesized peptide libraries could be improved by incorporating (i) cyclic structure and (ii) N-methylated amino acids in the backbone. Previously, we demonstrated that the ribosome could be used to construct N-methylated peptides and that these oligomers were highly resistant to protease degradation (20). Disulfide-based cyclization has been used extensively as a structural constraint in phage display libraries (21, 22) but is compromised by reduction in the intracellular environment (23). More recently, we designed and synthesized a trillion-member cyclic peptide library in mRNA display format using a bis-NHS cross-linking reagent to join the N-terminus to an internal lysine residue (24).

Here we describe cyclic mRNA display and employ it to design macrocyclic peptide ligands for Gαi1. These libraries were constructed with an expanded genetic code, using *N*-methylphenylalanine (NMF) as the 21st amino acid. The resulting cyclic peptides, such as cyclic Gαi binding peptide (cycGiBP), bind Gαi1 with monoclonal antibody-like affinity (K_d = 2.1 nM), the highest reported affinity for a small peptide ligand bound to a Gα subunit. This work presents a potentially general route to design cyclic peptide ligands against a broad range of protein targets.

METHODS

NMF-tRNA

The synthesis of *N*-methyl, *N*-nitroveratrylcarbonyl phenylalanine cyanomethyl ester was carried out according to the published protocol (20) with minor modifications. The final product was purified by silica gel chromatography in 1:1 EtOAc/hexanes. Yield = 187.5 mg (74%). Analysis by low-resolution electrospray ionization MS (ESI MS): $[M + Na]^+$ expected 479.15, observed 479.6.

The synthesis of *N*-methyl, *N*-nitroveratrylcarbonyl phenylalanine-dCA was carried out according to previous protocol. Yield = 0.5 mg (5.5%). Analysis by low-resolution ESI-MS: $[M - H]^-$ expected 1035.2, observed 1035.2.

Following ligation to THG-73 tRNA (30), deprotection of the nitroveratryloxycarbonyl group was effected by photolysis with a xenon lamp equipped with a 315-nm cutoff filter, and the NMF-tRNA was immediately added to the translation reaction.

Synthesis of $MX_{10}K$ Library

Antisense $MX_{10}K$ single-stranded DNA template was synthesized at the Keck Oligonucleotide Synthesis Facility (Yale) and the sequence is 5′… GCCAGACCCCGATTTSNNSNNSNNSNNSNNSNNSNNSNNSNNSNNCATTGTAATT GTAAATA-GTAATTG …3′, where N = A,T,C,G and S = G,C. The reagent bottle used for the "N" positions was made by mixing A:C:G:T in the ratio 3:3:2:2. The reagent bottle for "S" positions was made by mixing C:G in a 3:2 ratio.

$MX_{10}K$ library double-stranded DNA was amplified by five cycles of polymerase chain reaction (PCR) using the forward primer Gen-FP (5′-TAATACGACTCACTATAGGGACAATTACTATTTACAATTA CA-3′) and the reverse primer $MK^{10}K$-RP (5′…ACCGCTGCCAGACCCCGATT T…3′). The Round 0 mRNA pool was generated by T7 runoff transcription and purified by urea-PAGE. The purified mRNA was ligated to F30P (5′-$dA_{21}[C_9]_3$dAdCdC-P; C_9 = tri-(ethylene glycol) phosphate (Glen Research), P = puromycin (Glen Research)), *via* an oligonucleotide splint ($MX_{10}K$-splint: 5′… TTTTTTTTTTTTTACCGCTGCCAGAC …3′). Following PAGE purification of the ligation reaction, the template was dissolved in water and quantitated by absorbance at 260 nm.

Translation and Cyclization

Translation of the round 0 pool was aimed at generating an initial complexity of 1.67×10^{12} unique mRNA–peptide fusion sequences with 3-fold oversampling. Accordingly, 300 pmol of $MX_{10}K$ template was translated in rabbit reticulocyte lysate under standard conditions. The translation reaction was supplemented with 60 μg of NMF-$tRNA^{CUA}$ in 1 mM NaOAc (pH = 4.5) and ^{35}S-methionine. After 1 h of translation at 30 °C, KOAc and MgOAc were added to a final concentration of 600 and 50 mM, respectively, and the reactions were placed at −20 °C for 1 h.

Translation mixtures were diluted 1:10 in dT binding buffer (10 mg mL^{-1} dT cellulose, 1 M NaCl, 20 mM Tris, 1 mM EDTA, 0.2% (v/v) Triton X-100, pH = 8) and agitated for 1 h at 4 °C. The dT cellulose was filtered and washed with dT wash buffer (300 mM NaCl, 20 mM Tris, pH = 8). The DNA–peptide conjugates were eluted with 10 mM NH_4OH and ethanol precipitated in the presence of linear acrylamide (Ambion).

The round 0 pool was cyclized by adding 190 μL of dT-purified fusions in 50 mM phosphate buffer (pH = 8) to 50 μL of DSG (1 mg mL^{-1} in DMF). The reaction was allowed to proceed for 1 h, and the fusions were repurified by dT-cellulose and ethanol precipitated.

In subsequent rounds, 60 pmol of library template was translated in the presence of 12 μg of NMF-$tRNA^{CUA}$ in 1 mM NaOAc (pH = 4.5). Cyclization was performed by adding 40 μL of dT-purified fusions in 50 mM phosphate buffer (pH = 8) to 10 μL of DSG (1 mg mL^{-1} in DMF).

Selection

Following ethanol precipitation of the round 0 DSG-treated fusions, the pellet was dissolved in 100 μL of dH_2O (0.005% (v/v) Tween-20) and reverse transcribed with Superscript II RNase H^- under standard conditions. Following reverse transcription, the library was added to 5 mL of 1X selection buffer (25 mM HEPES-KOH (pH % 7.5), 150 mM NaCl, 0.05% (v/v) Tween-20, 1 mM EDTA, 5 mM $MgCl_2$, 1 mM β-mercaptoethanol, 10 μM GDP, 0.05% (w/v) bovine serum albumin, 1 μg mL^{-1} tRNA) containing 50 μL of Gαi1-NeutrAvidin agarose (preblocked with biotin) (5). The binding reaction was carried out at 4 °C for 1 h. The reaction was filtered, and the resin was washed four times with 1X selection buffer and twice with 1X selection buffer (−BSA, − tRNA) at 4 °C. The library was eluted with 0.15% (w/v) SDS at RT, and the SDS was removed from the sample using SDS-Out (Pierce). Following ethanol precipitation, the library was amplified by 15 cycles of PCR.

In subsequent rounds, the binding reaction was carried out in 1 mL of selection buffer containing 6 μL od Gαi1-NeutrAvidin agarose. PCR amplification of the eluted library members was carried until a 96-bp band was observed on a 4% agarose gel (11–14 cycles). The binding for each round was determined by adding 5 μL of radiolabeled library to 2 μL of Gαi1-NeutrAvidin agarose in 800 μL of 1X selection buffer. After 1 h at 4 °C, the resin was washed as described above and analyzed by scintillation counting to determine the fraction of counts bound.

Pool 7 Analysis

The round 7 pool was amplified by 12 cycles of PCR and purified using the MinElute PCR Purification Kit (Qiagen). The purified PCR product was subcloned into the PCR 4-TOPO vector (Invitrogen) followed by transformation into TOP10 competent cells (Invitrogen). Individual clones were sequenced (Laragen). Sequence analysis of the least conserved round 6 and 7 clones (positions 9, 10, and 11; 14 total clones) gave 132 “N” positions with compositions A = 22%, T = 17%, G = 20%, C = 41% and 66 G/C positions with compositions of G = 44% and C = 56%. The amino acid compositions tended to small/polar residues with S = 25%, A = 16%, Q = 16%, T = 16%, D = 6%, P = 5%, R = 5%, G = 5%, L = 1.5%, N = 1.5%, W = 1.5%, and C = 1.5%. The sequences were thus consistent with the idea that the original library was not badly biased.

Five clones (R7.2, R7.3, R7.4, R7.6, R7.12) were further amplified and used to generate templates for mRNA–peptide fusion formation as described above. Following translation in the presence of ^{35}S-methionine, fusions were treated with RNase cocktail (Ambion) for 15 min at 37 °C and purified by dT-cellulose and ethanol precipitation. The 16-μL aliquots of fusion (in 50 mM phosphate buffer) were treated with 4 μL of either DMF or DSG (1 mg mL^{-1}) in DMF and allowed to react at RT for 1 h. The reactions were quenched with NaOH, neutralized with HCl, and added directly to 900 μL of 1X selection buffer containing 3 μL of Gαi1-NeutrAvidin agarose (preblocked with biotin). After 1 h at 4 °C, the solid resin was washed twice in 1X selection buffer and once with 1X selection buffer (–BSA, –tRNA). The counts remaining on the Gαi1-NeutrAvidin-agarose were assayed by scintillation counting. The bulk library from round 7 was treated as described above and included as a positive control.

Synthesis of linGiBP-Bio and cycGiBP-Bio

linGiBP-Bio (MITWYEFVAGTKGG-Biotin) was synthesized by manual solid-phase peptide synthesis with 250mg of Biotin NovaTag resin (Novabiochem). Following deprotection, cleavage, filtration, and ether extraction, the crude product was purified on a Vydac C-18 reverse phase column using gradient elution (0% B for 5 min, 10–50% B in 30 min. Solvent A: 0.1% TFA. Solvent B: CH_3CN (0.035% B)). Lyophilized solid was

quantitated by absorbance at 280 nm (ε_{280} = 6970 L mol^{-1} cm^{-1}). Yield = 1.3%. Analysis by MALDI TOFMS: $[M + H]^+$ expected 1827.9, observed 1830.1.

The cyclization of linGiBP-Bio was carried out by adding 80 μL of DSG (4 mM in DMF) to linGiBP-Bio (320 nmol in 232 μL of 100 mM phosphate buffer). The reaction was allowed to proceed for 3 h at RT then quenched with 6 mL 0.1% TFA. R7.6-Bio was purified by C-18 RP-HPLC chromatography with gradient elution (0% B for 5 min, 20–60% B in 40 min. Solvent A: 0.1% TFA. Solvent B: CH_3CN (0.035% B)). Lyophilized solid was quantitated by absorbance at 280 nm (ε_{280} = 6970 L mol^{-1} cm^{-1}). Yield = 6.1%. Analysis by MALDI TOFMS: $[M + H]^+$ expected 1923.9, observed 1925.3.

Synthesis of linGiBP and cycGiBP

Synthesis and quantitation of linGiBP (MITWYEFVAGTK-$CONH_2$) was carried out as described above except that 500 mg of Rink amide resin (0.34 mmol capacity, Novabiochem) was used as the solid phase. Yield = 2.6%. Analysis by MALDI TOFMS: $[M + H]^+$ expected 1444.7, observed 1446.0.

A 2.8-μmol portion of linGiBP was dissolved in 2.1 mL of DMF and 3.4 μL of DIEA (19.6 μmol, 7 equiv). To this was added 77 μL of DSG (40 mM in DMF, 1.1 equiv). The reaction was stirred at RT for 3 h and poured into 10 mL of 4:1 dH_2O (0.1% TFA)/CH_3CN (0.035%TFA). cycGiBP was purified by C18 RP-HPLC chromatography under the conditions described above. Yield = 32%. Analysis by MALDI TOFMS: $[M + H]^+$ expected 1540.7, observed 1542.0.

Specificity Analysis of GiBP-Bio

TNT pulldown experiments were carried out as described in ref 4. Equal amounts of each radiolabeled subunit were added to 8 μL of NeutrAvidin-agarose containing 14 pmol of prebound linGiBP-Bio or cycGiBP-Bio in 600 μL of 1X selection buffer (+BSA, −tRNA). Control NeutrAvidin-agarose was treated with DMSO alone. Binding reactions proceeded for 1 h at 4 °C followed by filtration and washing with 1X selection buffer (+BSA, −tRNA). The matrix was analyzed by scintillation counting, and the percent bound was determined by the matrix counts divided by the total counts as determined by TCA precipitation.

R6A Competition/Equilibrium Binding

The relative binding affinities of R6A, linGiBP, and cycGiBP were determined by equilibrium competition experiments *versus* biotinylated R6A (Bio-R6A), and fits and midpoints were determined using GraphPad Prism 4.03 (31). Each concentration point was determined in triplicate, and two independent sets of experiments were conducted to determine values for cycGiBP. The midpoints were used to calculate relative binding free energies ($\Delta\Delta G°$) for R6A, linGiBP, and cycGiBP vs. Bio-R6A at the assay temperature (4 °C). Binding constants at 25 °C were determined using these ΔΔG° values, the known 25 °C K_d = 60 nM value for R6A (5), and the assumption that the $\Delta\Delta G°$ the values are constant over this temperature range (formally, this assumes the formation enthalpy ($\Delta H°_{formation}$) for each of the three peptide–Gαi1 complexes is the same or very similar over this range). The free energy effect of cyclization was determined by subtraction of the $\Delta\Delta G°$ values for linGiBP and cycGiBP. We estimate the precision for these values as ±0.3 kcal mol^{-1}. This procedure results in a K_d = 70 nM for the control non-biotinylated R6A, a systematic error of ~0.1 kcal mol^{-1}.

In the experiments, ^{35}S-labeled Gαi1 was incubated with Bio-R6A immobilized on NeutrAvidin beads (Promega) and varying concentrations of nonbiotinylated competitor peptide. The fraction of counts bound to Bio-R6A was then determined by pull down. R6A

(MSQTKRLDDQLYWWEYL) and Bio-R6A (Bio-MSQTKRLDDQLYWWEYL) were synthesized by previously described methods. ^{35}S-Labeled Gαi1 was expressed using the TNT reticulocyte lysate system (T7 promoter, Promega) and desalted using MicroSpin G-25 columns (GE Healthcare) into modified HBS-EP buffer [10 mM HEPES at pH 7.4, 150 mM NaCl, 3 mM EDTA, 0.005% (v/v) polysorbate 20 (Tween 20), 8 mM $MgCl_2$, 30 μM GDP, and 0.05% (w/v) BSA]. The total ^{35}S-labeled Gαi1 counts and specific activity were measured by TCA precipitation.

In each binding reaction, 400 pmol of immobilized R6A and ~50,000 cpm of Gαi1 were suspended in 1 mL of HBS-EP buffer, and varying quantities of free peptide (R6A-1, linGiBP, or cycGiBP) were added. In each reaction, the final DMSO concentration was adjusted to ~0.5% (v/v). Samples were rotated for 2–4 h at 4 °C followed by brief centrifugation and supernatant removal. Samples were washed four times by resuspension in modified HBS-EP buffer at 4 °C, centrifugation, and supernatant removal. After the final wash, the immobilized sample was transferred to scintillation vials and analyzed by scintillation counting.

Protease Resistance Experiment

linGiBP and cycGiBP (1.8 mM) in DMSO were added to 50 mM sodium phosphate buffer to a final concentration of 145 mM. Immobilized α-chymotrypsin agarose (Sigma) was added to a final concentration of 21.5 mU mL^{-1}. The reaction proceeded at RT for 40 min with agitation. A 100-μL sample was removed from the reaction at 0, 5, 10, 20, and 40 min and diluted in 500 mL of 0.1% TFA. The resulting samples were filtered and injected onto a C-18 reverse phase column and separated by gradient elution (0–40% B in 25 min. Solvent A: 0.1% TFA. Solvent B: CH_3CN (0.035% B)). The area under the starting material peak was quantitated using the 32 KaratGold Software package (Beckman). The plotted values represent the mean of three experimental value, and the error bars represent the standard error of the mean. The graph was generated by fitting the data to a one-phase exponential decay equation (GraphPad Prism 4.03 (31)).

RESULTS AND DISCUSSION

Selection for Binding to Gαi1

We began with a library of the form $MX_{10}K$, where X represents a random position encoded by an NNG/C codon. We had previously shown that a library of this general form could be cyclized with good efficiency by linking the N-terminus to the fixed lysine side chain *via* the bis-NHS reagent disuccinimidyl glutarate (DSG) (24). This work also demonstrated that it was possible to construct a trillion-member macrocyclic library containing an unnatural amino acid. In the present work, we combined these features to generate a trillion-member library containing NMF as the 21st amino acid.

This library was translated in the presence of amber-suppressor NMF-transfer RNA $(tRNA)^{CUA}$ and cyclized with DSG (Figure 1). The random region was constructed with 10 tandem NNS repeats, resulting in UAG (amber) stop codons at a frequency of ~3% at each of the random positions. The estimated diversity of the round 0 pool was 1.67×10^{12} unique sequences with ≥3 copies of each molecule. The library was panned against immobilized Gαi1, and the tightly binding sequences were amplified to generate the DNA for the subsequent round. The results of the selection are shown in Figure 2. The binding of each pool to the immobilized target began to increase in the fourth round and continued to increase until round 7. At this point, the library was sequenced; the results are shown in Figure 2, panel b. As can be seen from the sequence alignment, glutamic acid and phenylalanine are 100% conserved at positions 6 and 7, respectively. Tryptophan is found at

position 4 in seven of the eight sequences. Threonine or serine residues are found at position 3, and hydrophobic residues (leucine, isoleucine, or valine) are found at position 8. R7.4 and R7.5 are identical and represent the only sequence to appear twice in the round 7 pool. Interestingly, the TWYEFV hexamer sequence appears three times independently in pool 7 and represents a conserved coremotif similar to that observed in previous selection experiments (Table 1 and references therein).

Positions 9–11 show little consensus, although at least one serine or threonine is found in this region in all of the round 7 clones. This pattern was also observed in clones from the previous round (data not shown), implying that a hydrogen bond donor is required in this region, although its position within the sequence may not be strictly enforced. No lysine residues were observed within the randomized region, providing initial evidence that cyclization proceeds *via* cross-linking of the primary amines on the N-terminus and the side chain of Lys12.

It is striking that the conserved hexamer core motif (residues 3–8) remains in the same position within the random region in all of the clones under study. This may indicate that the location of the core motif within the macrocycle was optimized by the selection process and is critical for interaction with Gαi1.

We next screened individual clones for Gαi1 binding activity. Five pool 7 sequences were synthesized as ^{35}S-methionine radiolabeled mRNA–peptide fusions, and the RNA was removed to simplify the binding analysis. The individual fusions were then either cyclized with DSG or mock treated with DMF and tested (Figure 3). Two features can be observed in this data. First, treatment with DSG resulted in dramatically higher binding efficiencies in all of the clones. The ratio of binding efficiency between DSG-treated fusions and DMF-treated fusions ranged from 5-fold (R7.3) to 52-fold (R7.2). This result argues that cyclization played a key role in the selection of these molecules. Second, the average binding efficiency of the fusions treated with DSG ranged from 2.3% (R7.12) to 8.4% (R7.6), and the overall average binding for the individual DSG-treated fusions (4.7%) was similar to the binding efficiency for the entire DSG-treated round 7 pool (4.8%).

DSG-treated clone R7.6 was the most active fusion, with a binding efficiency of 8.4%, a 38-fold enhancement relative to the DMF-treated fusion. This clone was selected for further characterization. R7.12, the only clone to have a leucine instead of a tryptophan at position 4, showed the lowest binding efficiency. This tryptophan has been observed in other Gαi1-binding peptides (Table 1 and references therein) and argues for its importance for high-affinity binding. R7.2, R7.4, and R7.6 contain the same hexamer core motif (TWYEFV), yet the differences in their binding efficiencies implicate the importance of the non-conserved residues (position 2 and positions 9–11). These residues may increase or decrease the efficiency of cyclization or may play a more direct role in the interaction between the macrocycle and the Gαi1 target.

None of the clones from round 7 contained a TAG stop codon, indicating that NMF was excluded to some degree in the context of the cyclic peptide. Given the sequences in pool 7, this was somewhat surprising because it appears that NMF could have been incorporated at position 7 in place of phenylalanine or in the non-conserved residues (position 2 and positions 9–11). At position 7, the crystal structure of the closely related peptide KB-752 bound to Gαi1 (12) shows that the backbone amide of phenylalanine is situated to make intramolecular hydrogen bonds to maintain the α-helical character of the core motif. Incorporation of the N-methylated variant there would oblate these interactions and presumably destabilize the binding conformation of the peptide. At the non-conserved

positions, NMF may have been excluded by steric effects, the requirement for polar residues, or poor incorporation relative to natural residues.

Characterization of linGiBP-Bio and cycGiBP-Bio

To further characterize the R7.6 peptide, we constructed the molecule by 9-fluorenylmethyl carbamate based chemical synthesis. We began by constructing a biotinylated version of the linear peptide (MITWYEFVAGTKGG-Bio) to allow for immobilization and subsequent pull-down experiments (Figure 4, panel a). After purification and deprotection of the linear chain, we cyclized the peptide to form cycGiBP-Bio under similar conditions used for the bulk $MX_{10}K$ library during the selection (4:1 100 mM phosphate (pH = 8)/DMF) (Figure 4, panel b). Despite the fact that the peptide had no protecting groups, the reaction proceeded smoothly to completion in 1 h at RT without noticeable formation of side products (Figure 4, panel c).

We also constructed minimal versions of both linGiBP and cycGiBP lacking the C-terminal biotin and glycine spacer (Figure 4, panel b, bracketed portion). Removal of the biotin and polar C-terminal residues resulted in poor water solubility of linGiBP. This prompted us to perform cyclization in pure DMF using DIEA as the organic base to generate cycGiBP (Figure 4, panel b). The yield of cycGiBP obtained under organic reaction conditions was similar to that obtained for cycGiBP-Bio under aqueous reaction conditions.

Subunit and State Specificity of cycGiBP

We next worked to characterize the specificity of both the linGiBP-Bio and cycGiBP-Bio. To do this, each peptide was immobilized and used to determine binding to radiolabeled Gα subunits (Figure 5, panel a). As before, the binding efficiency with cycGiBP-Bio was dramatically greater than with the linear peptide. As with previously selected peptides, cycGiBP-Bio recognizes all three Gαi class members with almost identical efficiencies. This is not surprising given that Gαi1, Gαi2, and Gαi3 share >85% sequence identity at the amino acid level (25). Generally, cycGiBP-Bio shows selectivity better than that of peptides isolated to date using *in vitro* selection. For example cycGiBP-Bio binds ~10× more Gαi than Gαo, in contrast to R6A-1, which binds the two subunits equally. Similarly, cycGiBP shows no binding to Gαq, whereas R6A binds to this subunit and Gαi with comparable efficiency (4). The cyclic peptide showed less relative binding to Gαs than the unselective peptide KB-752 (12), consistent with previous data obtained with R6A-1 (4). From these experiments, we conclude that cycGiBP-Bio preferentially binds to subunits in the Gαi subclass with specificity comparable to that of Gαi-binding peptides previously selected with mRNA display. Finally, both the linear and cyclic peptides bind specifically to a single state of the G protein, the GDP-bound form of Gαi1. Little binding is seen to the activated form (bound to GTPγS) or a mimic of the GTP hydrolysis transition state (bound to GDP-AlF_4^-) (Figure 5, panel b).

Binding Affinity of linGiBP and cycGiBP

We next sought to determine the relative affinity of cycGiBP for Gαi1 binding using an equilibrium competition assay. The well-studied peptide R6A (K_d = 60 nM) was used as our control, and binding constants were determined relative to this standard. N-Terminally biotinylated R6A was immobilized on NeutrAvidin-agarose, and varying concentrations of free peptide (linGiBP, cycGiBP, or free R6A) were added along with limiting amounts of radiolabeled Gαi1 (Figure 6). This approach allowed us to determine relative binding constants for linGiBP and cycGiBP, as well as non-biotinlyated R6A itself. Both linGiBP and cycGiBP compete with the R6A for binding to Gαi1, supporting the idea that they bind to a common site on Gαi1. The linGiBP binds ~2-fold more tightly ($K_d \approx 31$ nM) than R6A, a very high affinity given the linGiBP's comparatively small size (12 residues). On the other

hand, this selection utilized 10 random residues, whereas R6A was originally designed from a library with only 6 random positions.

Analysis of cycGiBP was even more surprising, indicating that it binds ~30-fold tighter (K_d ≈ 2.1 nM) than R6A, an improvement in free energy of 2.0 kcal mol^{-1}. Comparing cycGiBP with the linear form, the cycle is improved ~15-fold, a $\Delta\Delta G$ of −1.6 kcal mol^{-1}. It seems likely that this enhancement is due primarily to the reduced conformational entropy of the cycle compared with linGiBP. Invoking a thermodynamic cycle, the enhancement in binding free energy for the peptide should be the same as the increase in folding stability induced by cyclization, provided the target interactions are the same for the cycle and the linear molecules. Previously, Deechongkit and Kelly (26) have measured the folding stabilization due to cyclization in a different system (27), and statistical mechanics has also been used to calculate the stabilization. Both efforts indicate that the stabilization is modest and varies with the nature of the linker. Deechongkit and Kelly report a maximal stabilization of 1.7 kcal mol^{-1}, in excellent agreement with our observed binding enhancement of 1.6 kcal mol^{-1}. This finding has two implications. First, it appears that selection has energetically optimized the position of the linker, as discussed previously. Second, this approach suggests that optimally one can expect a 15- to 20-fold increase in binding free energy upon cyclization of a linear peptide ligand. A comparison of the binding free energies of known Gαi1-GDP ligands is shown in Figure 6, panel b.

Finally, we determined the effect of cyclization on the proteolytic stability of GiBP. The linear and cyclic peptides were incubated with immobilized chymotrypsin at RT for 40 min, and the amount of starting material was measured at various time points by RP-HPLC (Figure 7, panel c). Cyclization increased the half-life from 3.7 to 9.7 min. Previous work with tripeptide-based cyclic peptidomimetic inhibitors of HIV protease reported complete resistance to cathepsin D and pepsin A degradation over the course of 1 h (28). However, for larger cyclic peptides it is not unreasonable to expect considerable proteolytic digestion within a 15-min time scale (29). In addition to demonstrating increased cyclic peptide stability, protease digestion of cycGiBP revealed a single product with $[M + H]^+ = 1558.5$, indicating the addition of 18 Da (Figure 7, panel b). This corresponds to the hydrolysis of a single bond within the macrocycle. Proteolysis of the linear peptide revealed two products with masses consistent with hydrolysis of the Tyr5–Glu6 bond (Figure 7, panel a). This finding is notable for two reasons. First, it provides additional evidence of a cyclic structure for cycGiBP. Second, we observe a single cleavage at the tyrosine–glutamic acid junction, despite there being three possible cleavage sites in cycGiBP (tryptophan–tyrosine, tyrosine–glutamic acid, and phenylalanine–valine). Thus, strategies that stabilize the tyrosine-glutamic acid amide bond could further enhance proteolytic stability.

In this work, we present the first selection of a redox-insensitive, post-translationally cyclized peptide using a biological display library with an expanded genetic code. The selected cyclic peptide showed specificity for the GDP-bound state of the Gαi1 and moderate specificity for the Gαi class. Competition experiments showed that cycGiBP bound to Gαi1 with extremely high affinity (K_i = 2.1 nM) and that cyclization resulted in a 15-fold improvement in binding affinity relative to the linear peptide. The cyclic peptide was also shown to have increased proteolytic stability relative to its linear counterpart. Taken together, cycGiBP represents an excellent lead compound for additional medicinal chemistry and *in vivo* studies. In the future, the use of cyclic, unnatural mRNA display libraries may enable the selection of high-affinity, high-specificity ligands with increased stability for biological applications.

Supplementary Material

Refer to Web version on PubMed Central for supplementary material.

Acknowledgments

We would like to than S. Ross for his help with molecular characterization of the GiBPs and B. Ja for his helpful advice in all aspects of the project. We thank T. Takahashi for his advice and assistance with DNA sequencing and N. Zacharias for synthesis of pdCpA. This work was supported by National Institutes of Health (NIH) GM R01 60416 (R.W.R.), NIH R21 GM 76678 (R.W.R.), and the Charles Lee Powell Foundation.

REFERENCES

1. Hopkins AL, Groom CR. The druggable genome. Nat. Rev. Drug Discovery. 2002; 1:727–730.
2. Cheng MM, Cuda G, Bunimovich YL, Gaspari M, Heath JR, Hill HD, Mirkin CA, Nijdam AJ, Terracciano R, Thundat T, Ferrari M. Nanotechnologies for biomolecular detection and medical diagnostics. Curr. Opin. Chem. Biol. 2006; 10:11–19. [PubMed: 16418011]
3. Roberts RW, Szostak JW. RNA-peptide fusions for the in vitro selection of peptides and proteins. Proc. Natl. Acad. Sci. U.S.A. 1997; 94:12297–12302. [PubMed: 9356443]
4. Ja WW, Adhikari A, Austin RJ, Sprang SR, Roberts RW. A peptide core motif for binding to heterotrimeric G protein alpha subunits. J. Biol. Chem. 2005; 280:32057–32060. [PubMed: 16051611]
5. Ja WW, Roberts RW. In vitro selection of state-specific peptide modulators of G protein signaling using mRNA display. Biochemistry. 2004; 43:9265–9275. [PubMed: 15248784]
6. Ja WW, Wiser O, Austin RJ, Jan LY, Roberts RW. Turning G proteins on and off using peptide ligands. ACS Chem. Biol. 2006; 1:570–574. [PubMed: 17168552]
7. McCudden CR, Hains MD, Kimple RJ, Siderovski DP, Willard FS. G-protein signaling: back to the future. Cell. Mol. Life Sci. 2005; 62:551–577. [PubMed: 15747061]
8. Overington JP, Al-Lazikani B, Hopkins AL. How many drug targets are there? Nat. Rev. Drug Discovery. 2006; 5:993–996.
9. Weinstein LS, Chen M, Xie T, Liu J. Genetic diseases associated with heterotrimeric G proteins. Trends Pharmacol. Sci. 2006; 27:260–266. [PubMed: 16600389]
10. Radhika V, Dhanasekaran N. Transforming G proteins. Oncogene. 2001; 20:1607–1614. [PubMed: 11313908]
11. Kimple RJ, Kimple ME, Betts L, Sondek J, Siderovski DP. Structural determinants for GoLoco-induced inhibition of nucleotide release by Galpha subunits. Nature. 2002; 416:878–881. [PubMed: 11976690]
12. Johnston CA, Willard FS, Jezyk MR, Fredericks Z, Bodor ET, Jones MB, Blaesius R, Watts VJ, Harden TK, Sondek J, Ramer JK, Siderovski DP. Structure of Galpha(i1) bound to a GDP-selective peptide provides insight into guanine nucleotide exchange. Structure. 2005; 13:1069–1080. [PubMed: 16004878]
13. Oxford GS, Webb CK. GoLoco motif peptides as probes of Galpha subunit specificity in coupling of G-protein-coupled receptors to ion channels. Methods Enzymol. 2004; 390:437–450. [PubMed: 15488193]
14. Finking R, Marahiel MA. Biosynthesis of nonribosomal peptides1. Annu. Rev. Microbiol. 2004; 58:453–488. [PubMed: 15487945]
15. Duplay, D. Physician's Desk Reference. 59th ed.. Montvale, NJ: Thompson PDR; 2005.
16. Burton PS, Conradi RA, Ho NF, Hilgers AR, Borchardt RT. How structural features influence the biomembrane permeability of peptides. J. Pharm. Sci. 1996; 85:1336–1340. [PubMed: 8961149]
17. Haviv F, Fitzpatrick TD, Swenson RE, Nichols CJ, Mort NA, Bush EN, Diaz G, Bammert G, Nguyen A, Rhutasel NS. Effect of N-methyl substitution of the peptide bonds in luteinizing hormone-releasing hormone agonists. J. Med. Chem. 1993; 36:363–369. [PubMed: 8381183]

18. Rezai T, Yu B, Millhauser GL, Jacobson MP, Lokey RS. Testing the conformational hypothesis of passive membrane permeability using synthetic cyclic peptide diastereomers. J. Am. Chem. Soc. 2006; 128:2510–2511. [PubMed: 16492015]
19. Veber DF, Freidinger RM. The design of metabolically-stable peptide analogs. Trends Neurosci. 1985; 8:392.
20. Frankel A, Millward SW, Roberts RW. Encodamers: unnatural peptide oligomers encoded in RNA. Chem. Biol. 2003; 10:1043–1050. [PubMed: 14652071]
21. Giebel LB, Cass RT, Milligan DL, Young DC, Arze R, Johnson CR. Screening of cyclic peptide phage libraries identifies ligands that bind streptavidin with high affinities. Biochemistry. 1995; 34:15430–15435. [PubMed: 7492543]
22. O'Neil KT, Hoess RH, Jackson SA, Ramachandran NS, Mousa SA, DeGrado WF. Identification of novel peptide antagonists for GPIIb/IIIa from a conformationally constrained phage peptide library. Proteins. 1992; 14:509–515. [PubMed: 1438188]
23. Gilbert H. Thiol/disulfide exchange equilibria and disulfide bond stability. Methods Enzymol. 1995; 251:8–28. [PubMed: 7651233]
24. Millward SW, Takahashi TT, Roberts RW. A general route for post-translational cyclization of mRNA display libraries. J. Am. Chem. Soc. 2005; 127:14142–14143. [PubMed: 16218582]
25. Strathmann M, Simon MI. G protein diversity: a distinct class of alpha subunits is present in vertebrates and invertebrates. Proc. Natl. Acad. Sci. U.S.A. 1990; 87:9113–9117. [PubMed: 2123549]
26. Deechongkit S, Kelly JW. The effect of backbone cyclization on the thermodynamics of β-sheet unfolding: stability optimization of the PIN WW domain. J. Am. Chem. Soc. 2002; 124:4980–4986. [PubMed: 11982361]
27. Zhou HX. Effect of backbone cyclization on protein folding stability: chain entropies of both the unfolded and the folded states are restricted. J. Mol. Biol. 2003; 332:257–264. [PubMed: 12946362]
28. March DR, Abbenante G, Bergman DA, Brinkworth RI, Wickramasinghe W, Begun J, Martin JL, Fairlie DP. Substrate-based cyclic peptidomimetics of Phe-Ile-Val that inhibit HIV-1 protease using a novel enzyme-binding mode. J. Am. Chem. Soc. 1996; 118:3375–3379.
29. Botti P, Pallin TD, Tam JP. Cyclic peptides from linear unprotected peptide precursors through thiazolidine formation. J. Am. Chem. Soc. 1996; 118:10018–10024.
30. Saks ME, Sampson JR, Nowak MW, Kearney PC, Du F, Abelson JN, Lester HA, Dougherty DA. An engineered Tetrahymena tRNAGln for in vivo incorporation of unnatural amino acids into proteins by nonsense suppression. J. Biol. Chem. 1996; 271:23169–23175. [PubMed: 8798511]
31. Motulsky, HC.; Christopoulos, A. Fitting Models to Biological Data using Linear and Nonlinear Regression. A Practical Guide to Curve Fitting. New York: Oxford University Press; 2004.
32. Rebois RV, Schuck P, Northup JK. Elucidating kinetic and thermodynamic constants for interaction of G protein subunits and receptors by surface plasmon resonance spectroscopy. Methods Enzymol. 2002; 344:15–42. [PubMed: 11771379]
33. Crooks GE, Hon G, Chandonia J-M, Brenner SE. WebLogo: a sequence logo generator. Genome Res. 2004; 14:1188–1190. [PubMed: 15173120]

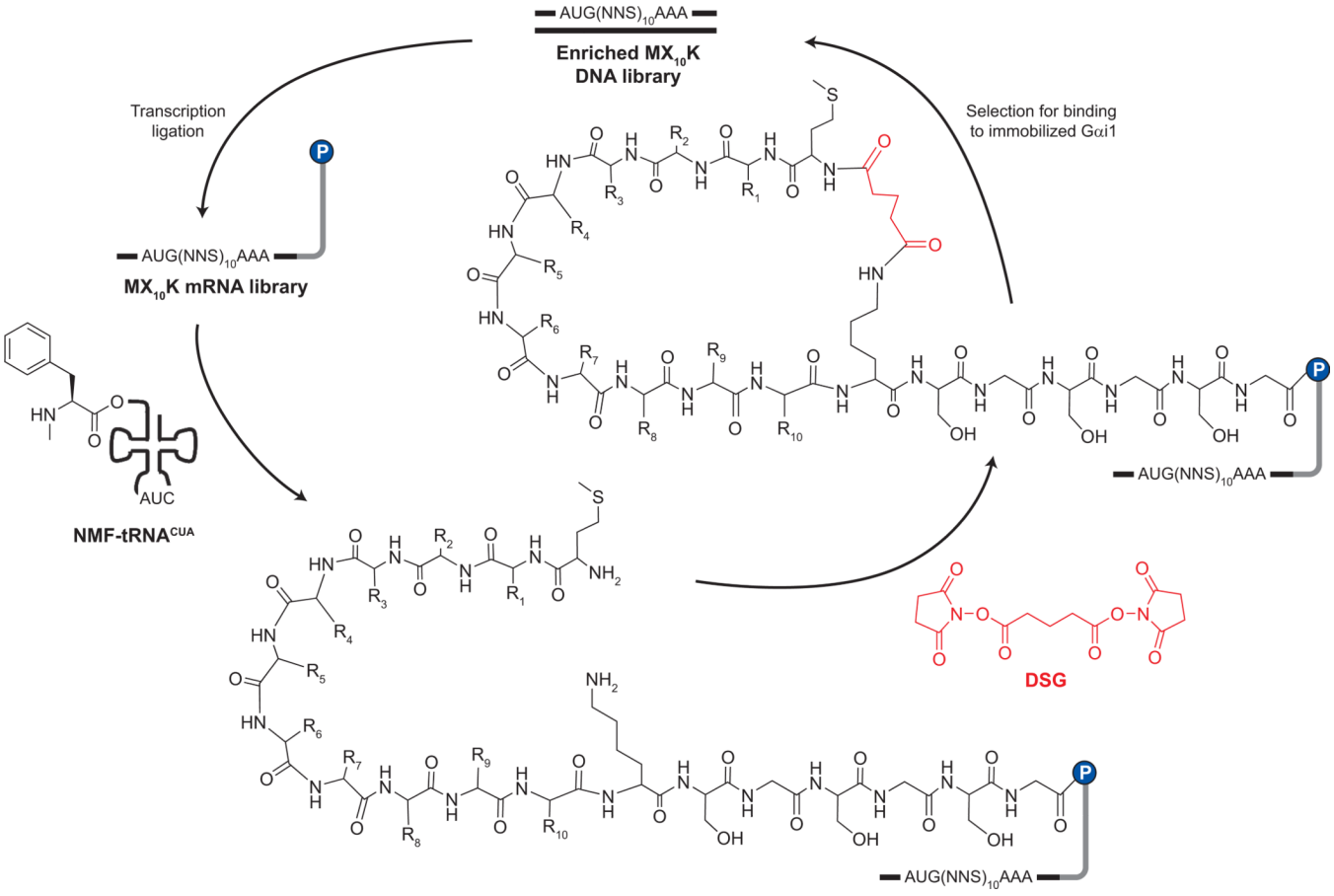

Figure 1.

Schematic of cyclic mRNA display selection. The $MX_{10}K$ library was transcribed from synthetic DNA and ligated to a short DNA linker (gray). The resulting template was translated in rabbit reticulocyte lysate in the presence of THG73 amber suppressor tRNA chemically aminoacylated with NMF ($NMF\text{-}tRNA^{CUA}$). The resulting mRNA–peptide fusion library was purified and cyclized with DSG. Members of the library that bound to the immobilized Gαi1 were eluted with SDS, and the corresponding sequences were amplified and enriched by PCR.

Figure 2.

Selection against Gαi1 using the $MX_{10}K$ library. a) The progress of the selection was monitored by measuring the fraction of radiolabeled library bound to NeutrAvidin-immobilized Gαi1 or NeutrAvidin alone. Initial selection rounds were carried out at 4 °C, and rounds 6 and 7 were performed at RT. b) Peptide sequences of clones obtained from pool 7. Residues that are conserved in all of the clones appear in red. The conserved hexamer core motif is shaded in gray. c) WebLogo (33) representation of pool 7 consensus sequence.

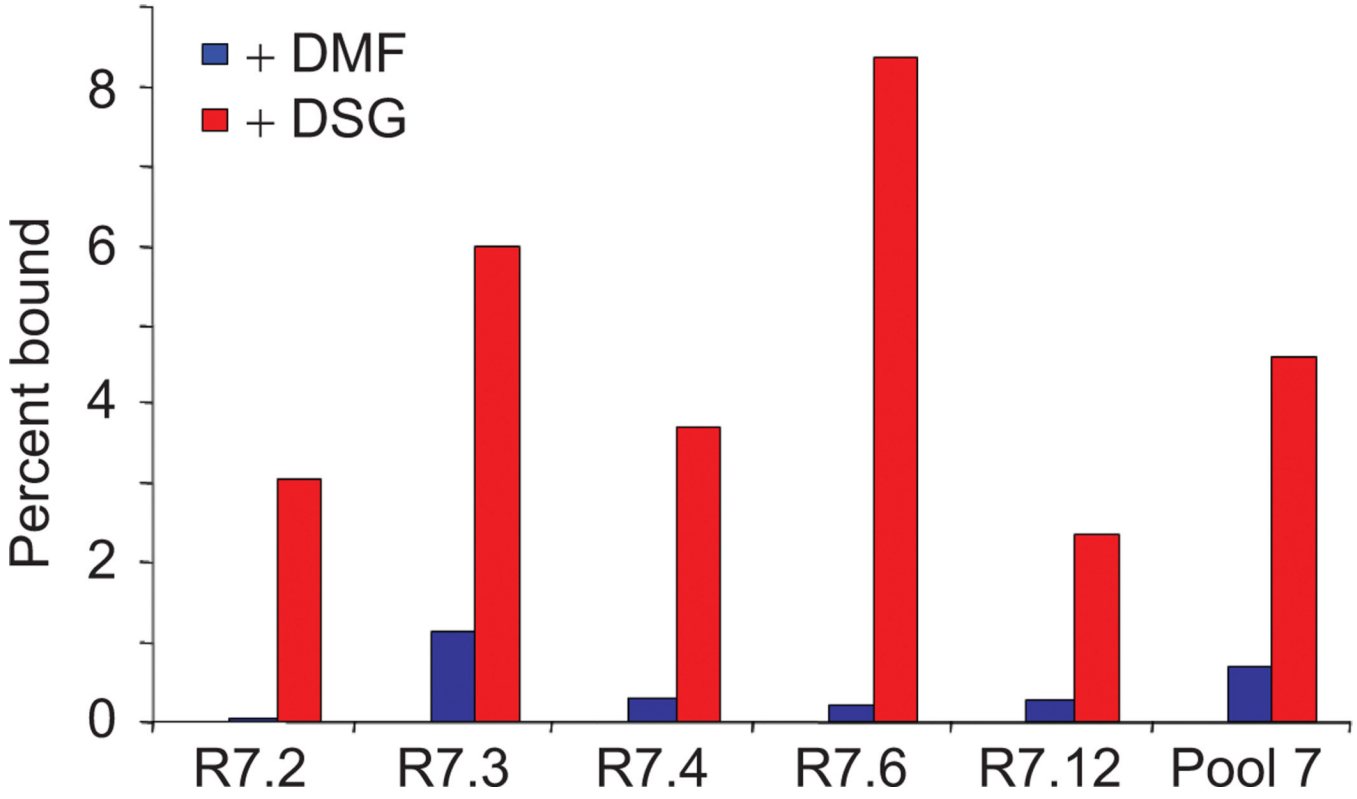

Figure 3.

Binding of radiolabeled pool 7 peptide fusions to immobilized Gαi1. Following translation, RNase treatment, and purification, the fusions were treated with either DMF or DSG for 1 h and assayed for binding. The percent bound values were taken from single experiments.

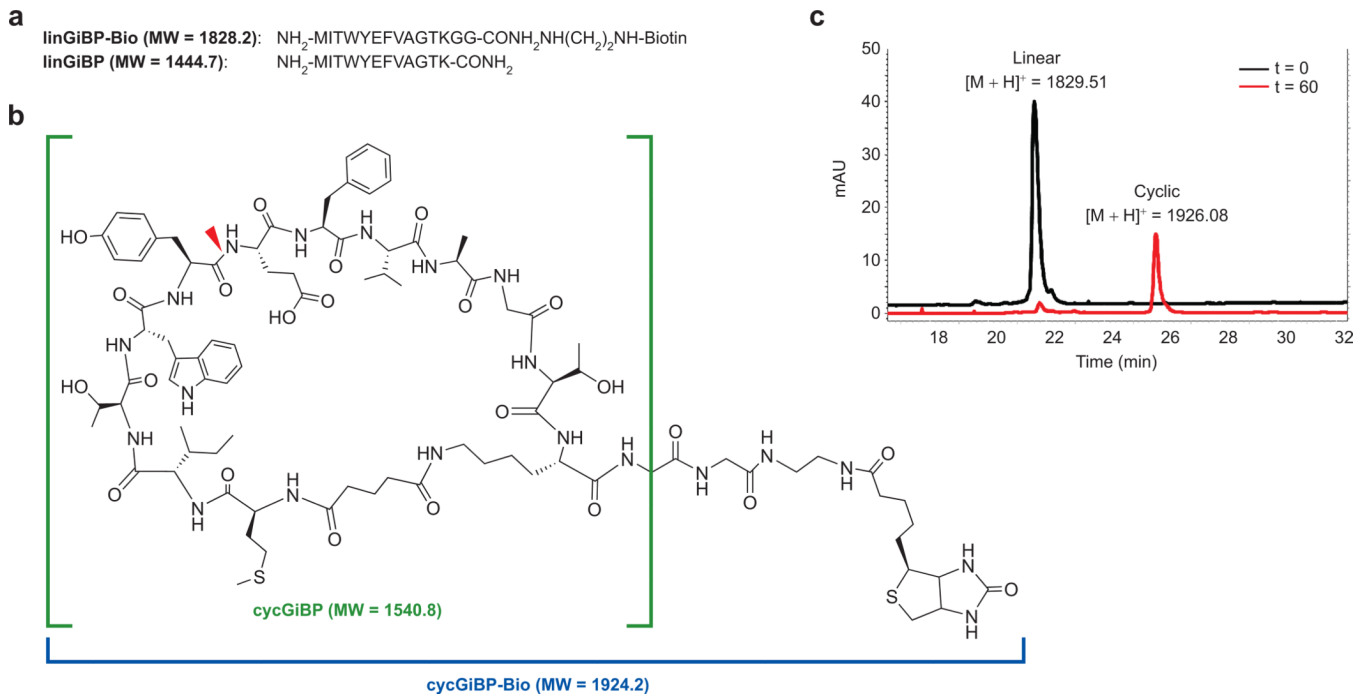

Figure 4.

Design and synthesis of peptides derived from R7.6. a) The peptide sequences of linGiBP and linGiBP-Bio. b) The structures of cycGiBP and cycGiBP-Bio. The location of the observed chymotrypsin digestion site is shown (red wedge). c) HPLC traces of the DSG-mediated cyclization reaction of the linGiBP-Bio peptide. At $t = 0$ and $t = 60$ min a portion of the reaction was separated on a C-18 reverse phase column and monitored by absorbance at 280 nm.

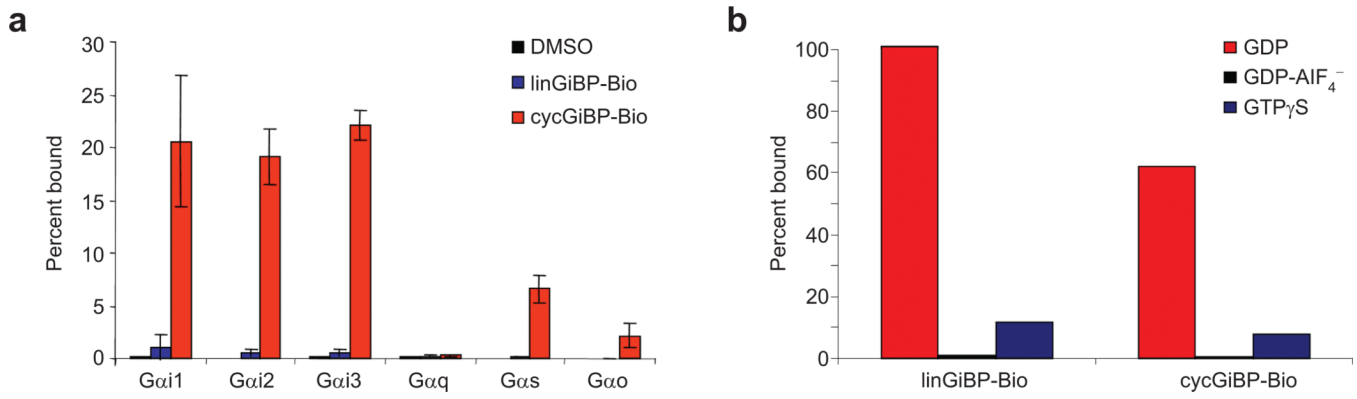

Figure 5.

Binding of radiolabeled Gα subunits to immobilized R7.6 peptides. a) NeutrAvidin-agarose was pretreated with DMSO, linGiBP-Bio, or cycGiBP-Bio and incubated with various radiolabeled Gα subunits. The percent bound values represent the mean value from three experiments, and the error bars represent the standard deviation. b) Nucleotide state specificity of GiBPs. linGiBP-Bio and cycGiBP-Bio were immobilized on NeutrAvidin and incubated with radiolabeled Gαi1 prebound with GDP, GDP-AlF_4^-, or GTPγS. The higher pull-down efficiency of linGiBP-Bio *vs* cycGiBP-Bio is due to the high level of linear peptide used (300 *vs* 15 pmol). The percent bound values were taken from single experiments.

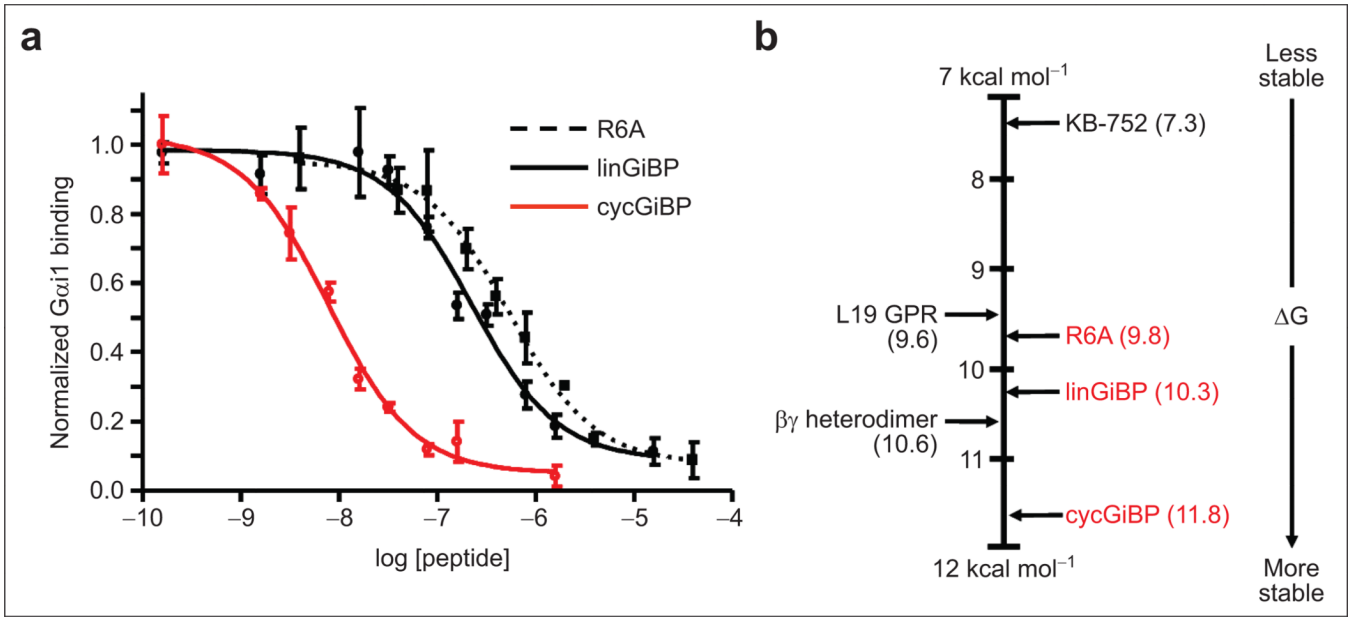

Figure 6.

Inhibition of radiolabeled Gαi1 binding to immobilized R6A peptide. a) Radiolabeled Gαi1 was incubated with immobilized biotinylated R6A and varying concentrations of either R6A, linGiBP, or cycGiBP for 2 h at 4 °C, and the radiolabel bound was normalized to that which bound in the absence of ligand. The plotted values represent the mean of three experimental values, and the error bars correspond to the standard deviation. b) Relative energetics of various peptide and protein interactions with GDP-Gαi1 at 25 °C. Values shown in black are calculated from the K_d values obtained from the literature (Table 1), whereas those in red were calculated from the dissociation constants described in this work. ΔG values are given in kcal mol^{-1}.

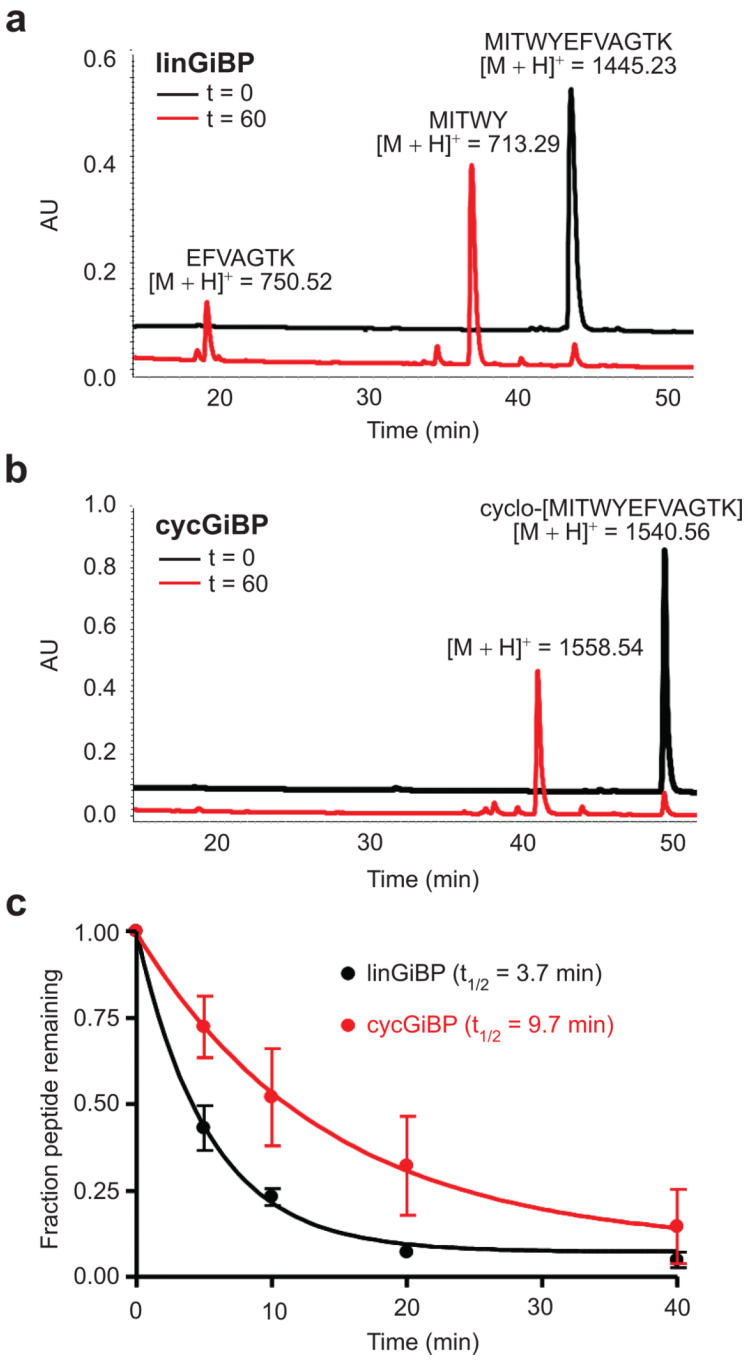

Figure 7.

Proteolysis of linGiBP and cycGiBP. linGiBP (a) or cycGiBP (b) were incubated with chymotrypsin for 60 min. The major products at $t = 0$ and $t = 60$ min were collected and analyzed by MALDI TOFMS. (c) Time course of chymotrypsin digestion.

TABLE 1

Natural and selected peptides that bind to Gαi subunits[a]

Peptide/protein	Sequence	MW(Da)	K_d (nM)	Reference
L19 GPR (GoLoco Motif)	TMGEEDFFDLLAKSQSKRLDDQLVDLAGYK	3433.8	82	5
KB-752	SRV**TWYDFL**MEDTKSR	2034.3	3900	12
R6A	MSQTKRLDDQL**YWWEYL**	2275.6	60	5
AR6-05	DESDPEELM**YWWEFL**SEDPSS	2591.7	10	6
linGiBP	MI**TWYEFV**AGTK	1444.7	31	*b*
cycGiBP	*cyclo*[MI**TWYEFV**AGTK]	1540.8	2.1	*b*
Gβγ	Heterodimer	~43,000	15	32

[a]The Gαi1-binding conserved core motif sequence is shown in bold. The K_d values for linGiBP and cyclic cycGiBP were obtained relative to R6A by equilibrium competition experiments (Figure 6) performed as described in Methods.

[b]This work.